Reliability of Initially Compressed Uncertain Laminated Plates in Supersonic Flow

D. G. Liaw* and Henry T. Y. Yang†
Purdue University, West Lafayette, Indiana 47907

A stochastic thin-plate finite element is formulated to study the reliability of initially compressed laminated thin plates with structural uncertainties due to variabilities occurring during the fabricating process. The two failure criteria considered are buckling and supersonic flutter. Interactive effects between the in-plane load and aerodynamic pressure for the uncertain plates are also studied. For buckling analysis the structural uncertainties include the modulus of elasticity, thickness, and fiber orientation of individual lamina, as well as geometric imperfections of the entire plate. For flutter analysis additional uncertainties of mass density of plates, amplitudes of uniformity and linearly distributed in-plane loads, and air density are also considered. The formulation for the deterministic 16-degree-of-freedom quadrilateral laminated thin-plate element is based on the classical lamination theory. The stochastic element formulation is accomplished by including the effects of structural uncertainties and random in-plane loads. The stochastic solution procedure is developed based on the mean-centered second-moment perturbation technique. To evaluate the validity and demonstrate the applicability of the present developments, a series of vibration, buckling, and supersonic flutter analyses of thin plates with structural uncertainties under random in-plane loads was performed. The results quantify the effects of these uncertain parameters on the reduction of the structural reliability and stability boundary of initially compressed laminated plates. The results also provide physical insight into such practical design and fabrication problems.

Introduction

THIN plates are a popular and useful form of structural components, with many significiant applications in aerospace and other fields of engineering. For obvious advantages such as the high strength-to-weight ratio and high stiffness-to-weight ratio, fiber-reinforced laminated composite plates have been increasingly used in thin wall structures. Because of the difficulty frequently encountered in achieving top quality control of manufacturing process, structural variabilities may occur and are random in nature. These process-induced variabilities may include fiber size, volume fraction of fibers, fiber orientations, thickness of each lamina, and curvature of the plate. Such variabilities will affect the achievable performance of strengths and stiffness of the finished plates and will also influence their structural reliabilities.

It is a major objective of this study to investigate the effects of several random structural uncertainties on buckling and supersonic flutter behaviors as well as on the reliabilities of laminated thin plates. The random structural uncertainities considered include modulus of elasticity, mass density, thickness, and fiber orientation of individual lamina, as well as initial geometric imperfections of the entire plate.

In the design of thin-plate structures, such as a panel in a wing, it is often necessary to consider the effect of in-plane stresses. Such an effect on the natural frequencies was studied previously by, among others, Mei and Yang.[1] Such an effect on the critical aerodynamic pressure or flutter speed was also studied previously by, among others, Bisplingghoff and Ashley,[2] Sander et al.,[3] and Yang and Han.[4] It is apparently interesting to study further the effect of in-plane stress as a random variable on the critical aerodynamic pressure or flutter speed of the laminated thin plates. Such a study is another objective of this paper.

Studies of the uncertain structural parameters have focused primarily on the effects of imperfections on vibration and buckling of thin wall structures. In 1962, Bolotin[5] studied the buckling of cylindrical shells with random initial imperfections. Amazigo investigated the buckling of long cylindrical shells under axial compression[6] and external pressure[7] using the truncated hierarchy method and perturbation method, respectively. Van Slooton and Soong[8] treated the buckling of long cylindrical shells under axial compression using a perturbation technique developed by Dym and Hoff.[9] Scher Fersht[10] studied the buckling of long cylindrical shells with asymmetric random imperfections using the truncated hierarchy method. Elishakoff and Arbocz analyzed axially compressed cylindrical shells with axisymmetric[11] and asymmetric[12] imperfections using the Monte Carlo simulation method and the first-order second-moment approach.[13]

In recent years the interest in random uncertainties has been extended beyond the random geometric imperfections to include other possible uncertainties, such as modulus of elasticity, mass density, thickness, and fiber orientations. For example, Lawrence[14] analyzed isotropic plates with uncertain thickness under deterministic loads. Nakagiri et al.[15] studied the natural frequencies of laminated plates with uncertain fiber orientations.

It appears that in most previous studies only a single structural uncertain parameter was considered, with random geometric imperfection attracting the most attention. However, it is important and desirable to consider the combined effects of several essential structural uncertainties in the analysis, design, and safety assessment of structures. Such an idea was proposed[16,17] for the probabilistic seismic safety study of an existing nuclear power plant.

In this study a 16-dof quadrilateral stochastic laminated thin-plate element and a solution procedure within the framework of stochastic finite element method[18,19] are developed. The plate is assumed to be thin; hence, the classical lamination theory is applicable. The effect of the transverse shear deformations is neglected. The aerodynamic pressure due to supersonic potential flow is described by the two-dimensional quasi steady supersonic theory, which is also called the piston theory.[2] The effect of structural and aerodynamic damping on the determination of the characteristic of the flutter boundary was studied previously by, among others, Librescu and Badoiu.[20]

Received Dec. 27, 1989; revision received June 22, 1990; accepted July 5, 1990.

*Graduate Research Assistant, School of Aeronautics and Astronautics.

†Professor of Aeronautics and Astronautics and Dean of Schools of Engineering. Fellow AIAA.

The structural and aerodynamic nonlinearities also have a significant effect on the determination of the flutter characteristic. Such an effect has been studied by, among others, Librescu[21,22] and Han and Yang.[23] The formulation includes the linear stiffness, incremental stiffness, mass, and aerodynamic matrices. These matrices are random in nature, depending on the probabilistic properties of the uncertainties. The solution procedure is developed based on the mean-centered second-moment perturbation technique.

To establish the validity of the present stochastic finite element formulation and solution procedure, two examples, including an isotropic cantilever plate with uncertain modulus of elasticity and mass density and a simply-supported rectangular laminated composite plate with uncertain fiber orientation, are first solved and then compared with existing alternative solutions. To demonstrate the practical applicability of the present method in simultaneously treating a variety of structural uncertainties, a series of buckling, supersonic flutter, and reliability analyses of thin plates with uncertain modulus of elasticity, mass density, thickness, fiber orientations, and random imperfections under random in-plane loads is performed. Some representative results are varified by the Monte Carlo simulation approach. The results quantify the effects of these uncertain parameters on the reduction of the structural reliability and stability boundary of initially stressed laminated plates. The results also provide physical insight into such practical design and fabrication problems.

Formulation

Equations of Motion

The equations of motion for free vibration of a plate finite element subjected to in-plane force and aerodynamic pressure may be written as

$$[m]\{\ddot{q}\} + ([k]) + [n] + [a])\{q\} = \{0\} \tag{1}$$

where $[m]$, $[k]$, $[n]$, and $[a]$ are the consistent mass, linear stiffness, incremental stiffness, and aerodynamic matrices, respectively. The consistent mass, linear stiffness, and incremental stiffness matrices can be obtained by following a general procedure outlined in common text.[24] The aerodynamic matrix can be derived by following the procedure proposed by, among others, Sander et al.[3] and Yang and Han.[4]

In this study the aerodynamic matrix is formulated based on the two-dimensional quasisteady supersonic flow theory. The Mach number is limited to approximately beyond 1.6. The effect of random disturbances of the flow speed is not considered.

Random Structural Uncertainties

The random field of a single structural uncertainty is described as a random amplitude multiplied by a deterministic spatial function. The random amplitude ξ_i can be expressed as the sum of its mean value $E[\xi_i]$ and an random variable α_i as

$$\xi_i = E[\xi_i] + \alpha_i \tag{2}$$

The mean value of random variable α_i is equal to zero; thus, it has the same standard deviation as ξ_i.

After substituting Eq. (2) into the explicit forms of the element matrices for linear stiffness $[k]$, incremental stiffness $[n]$, mass $[m]$, and aerodynamic force $[a]$ and truncating the third- and higher-order terms, the stochastic formulation including the effects of structural uncertainties and in-plane forces can be obtained in terms of random variables α_i ($i = 1, 2, .., p$) in the following general form:

$$[c] = [c^{(0)}] + \sum_{r=1}^{p} [c_r^{(1)}]\alpha_r + \frac{1}{2}\sum_{r=1}^{p}\sum_{s=1}^{p} [c_{rs}^{(2)}]\alpha_r\alpha_s \tag{3}$$

where p is the total number of random variables in the element. The detailed deviation and the explicit forms for the element matrices can be found in the first author's Ph.D. dissertation.[25]

Solution Procedure for the Probabilistic Eigenvalue and Eigenvector Problem

The governing equation of a general eigenvalue problem is given in the following form:

$$([A] - \lambda[B])\{\Phi\} = \{0\} \tag{4}$$

where $[A]$ and $[B]$ are square matrices, λ is the eigenvalue of the system, and $\{\Phi\}$ is the right-hand side eigenvector corresponding to λ. The left-hand side eigenvector $\{\Psi\}$ corresponding to λ is such that

$$\{\Psi\}^T([A] - \lambda[B]) = \{0\} \tag{5}$$

It is noted that $\{\Phi\}$ equals $\{\Psi\}$ when both matrices $[A]$ and $[B]$ are symmetric. For the free vibration analysis matrices $[A]$ and $[B]$ represent matrices $[K]$ and $[M]$, respectively. For the buckling analysis matrices $[A]$ and $[B]$ represent matrices $[K]$ and $[N]$, respectively. For the flutter analysis matrices $[A]$ and $[B]$ represent the sum of the matrices $[K]$, $[N]$, and $[A_e]$, and the matrix $[M]$, respectively.

The matrices $[A]$ and $[B]$ are expanded with respect to the random variables α_i ($i = 1, 2, ..., m$) that represent the uncertainties involved in the system, respectively, as

$$[A] = [A^{(0)}] + \sum_{r=1}^{m} [A_r^{(1)}]\alpha_r + \frac{1}{2}\sum_{r=1}^{m}\sum_{s=1}^{m} [A_{rs}^{(2)}]\alpha_r\alpha_s \tag{6}$$

and

$$[B] = [B^{(0)}] + \sum_{r=1}^{m} [B_r^{(1)}]\alpha_r + \frac{1}{2}\sum_{r=1}^{m}\sum_{s=1}^{m} [B_{rs}^{(2)}]\alpha_r\alpha_s \tag{7}$$

where m is the total number of random variables in the system. The eigenvalues, right-hand eigenvectors, and left-hand eigenvectors are influenced by the uncertainties in the system and possess the similar expressions, respectively, as

$$\lambda = \lambda^{(0)} + \sum_{r=1}^{m} \lambda_r^{(1)}\alpha_r + \frac{1}{2}\sum_{r=1}^{m}\sum_{s=1}^{m} \lambda_{rs}^{(2)}\alpha_r\alpha_s \tag{8}$$

$$\{\Phi\} = \{\Phi^{(0)}\} + \sum_{r=1}^{m} \{\Phi_r^{(1)}\}\alpha_r + \frac{1}{2}\sum_{r=1}^{m}\sum_{s=1}^{m} \{\Phi_{rs}^{(0)}\}\alpha_r\alpha_s \tag{9}$$

and

$$\{\Psi\} = \{\Psi^{(0)}\} + \sum_{r=1}^{m} \{\Psi_r^{(1)}\}\alpha_r + \frac{1}{2}\sum_{r=1}^{m}\sum_{s=1}^{m} \{\Psi_{rs}^{(2)}\}\alpha_r\alpha_s \tag{10}$$

Substituting Eqs. (6–10) into Eqs. (4) and (5), truncating the third- and fourth-order terms, and equating equal-order terms, the zero-, first-, and second-order equations for the right-hand and left-hand side eigenvectors are obtained, respectively.

For zero orders

$$([A^{(0)}] - \lambda^{(0)}[B^{(0)}])\{\Phi^{(0)}\} = \{0\} \tag{11}$$

and

$$\{\Psi^{(0)}\}^T([A^{(0)}] - \lambda^{(0)}[B^{(0)}]) = \{0\} \tag{12}$$

For first order,

$$([A^{(0)}] - \lambda^{(0)}[B^{(0)}])\{\Phi_r^{(1)}] + ([A_r^{(1)}] - \lambda_r^{(1)}[B^{(0)}] - \lambda^{(0)}[B_r^{(1)}])\{\Phi^{(0)}\} = \{0\}, \qquad r = 1, 2, ..., m \tag{13}$$

and

$$\{\Psi_r^{(1)}\}^T([A^{(0)}]-\lambda^{(0)}[B^{(0)}]) + \{\Psi^{(0)}\}^T([A_r^{(1)}]-\lambda_r^{(1)}[B^{(0)}] - \lambda^{(0)}[B_r^{(1)}])=\{0\}, \qquad r=1, 2, \ldots, m \tag{14}$$

For second order,

$$([A^{(0)}]-\lambda^{(0)}[B^{(0)}])\{\Phi_{rs}^{(2)}\} + ([A_{rs}^{(2)}]-\lambda_{rs}^{(2)}[B^{(0)}]-\lambda_r^{(1)}[B_s^{(1)}] - \lambda^{(0)}[B_{rs}^{(2)}])\{\Phi^{(0)}\} + ([A_r^{(1)}]-\lambda_r^{(1)}[B^{(0)}] - \lambda^{(0)}[B_r^{(1)}])\{\Phi_s^{(1)}\}=\{0\}, \qquad r, s=1, 2, \ldots, m \tag{15}$$

and

$$\{\Psi_{rs}^{(2)}\}^T([A^{(0)}]-\lambda^{(0)}[B^{(0)}]) + \{\Psi^{(0)}\}^T([A_{rs}^{(2)}]-\lambda_{rs}^{(2)}[B^{(0)}] - \lambda_r^{(1)}[B_s^{(1)}]-\lambda^{(0)}[B_{rs}^{(2)}]) + \{\Psi_r^{(1)}\}^T([A_s^{(1)}] - \lambda_s^{(1)}[B^{(0)}]-\lambda^{(0)}[B_s^{(1)}])=\{0\}, \qquad r, s=1, 2, \ldots, m \tag{16}$$

Several methods have been proposed[15,26-28] to solve these equations based on different criteria for the normalization of the eigenvectors. After obtaining the zero-, first-, and second-order eigenvalues and eigenvectors, the mean values and the covariances of eigenvalues, right-hand side eigenvectors, and left-hand side eigenvectors can be calculated from Eqs. (8-10), respectively. For example, the mean value and the variance of the eigenvalue λ can be obtained by taking the expected values of λ and $(\lambda-\lambda^{(0)})^2$ from Eq. (8), respectively, as

$$E[\lambda]=\lambda^{(0)}+\frac{1}{2}\sum_{r=1}^{m}\sum_{s=1}^{m}\lambda_{rs}^{(2)}E[\alpha_r\alpha_s] \tag{17}$$

$$\sigma^2[\lambda]=E[(\lambda-E[\lambda])^2]\approx\sum_{r=1}^{m}\sum_{s=1}^{m}\lambda_r^{(1)}\lambda_s^{(1)}E[\alpha_r\alpha_s] \tag{18}$$

where $E[\alpha_r\alpha_s]$ is the covariance of random variables α_r and α_s and is described by the given probabilistic properties of structural uncertainties.

Results

To evaluate the present stochastic finite element formulation and solution procedure, obtain results to quantify the effects of the various uncertain parameters, and gain physical insight into the subject problems, a series of vibration, buckling, and supersonic flutter analyses and reliability study of thin plates with structural uncertainties under in-plane loads was performed. Interactive effects between the in-plane load and the aerodynamic pressure were also studied.

In all of the examples a sufficiently fine Gauss grid (5×5) was used for numerical integration to obtain the element linear stiffness, incremental stiffness, mass, and aerodynamic matrices. All calculations were done using a CYBER 205 vectorized supercomputer at Purdue University.

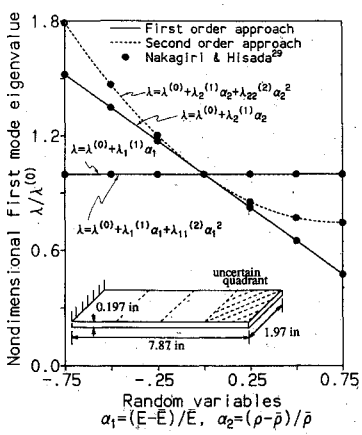

Fig. 1 First-mode eigenvalues of a cantilever plate with uncertain modulus of elasticity and mass density in a quadrant at the free end.

Vibration of an Isotropic Cantilever Plate with Uncertain Material Properties

The free vibration of an isotropic cantilever plate with uncertain modulus of elasticity and mass density was first studied. As shown in Fig. 1, the plate has a length of 7.87 in., a width of 1.97 in., and a thickness of 0.197 in. The material properties of the left three-quarters of the plate were assumed to be deterministic with modulus of elasticity of 30×10^6 psi and mass density of 0.728×10^{-3} lb-s^2/in.^{4}. The material properties of the right quarter of the plate were assumed to be uncertain. The mean values of the modulus of elasticity and mass density were assumed to be $\bar{E}=30\times10^6$ psi and $\bar{\rho}=0.728\times10^{-3}$ lb-s^2/in.^{4}, respectively. The uncertainties of the material properties were described by two random variables, α_1 and α_2, as

$$\alpha_1=(E-\bar{E})/\bar{E} \tag{19}$$

and

$$\alpha_2=(\rho-\bar{\rho})/\bar{\rho} \tag{20}$$

where E and ρ are the modulus of elasticity and the mass density, respectively.

Four elements were used to model the whole plate. Figure 1 shows the results for the nondimensional first-mode eigenvalues $\lambda/\lambda^{(0)}$ within the range $-0.75\le\alpha_1$ (or α_2) ≤0.75, where $\lambda^{(0)}$ is the first-mode eigenvalue for $\alpha_1=\alpha_2=0$. Both the first- and second-order approaches were used. The results obtained previously by Nakagiri and Hisada[29] using four elements are also plotted in Fig. 1 for comparison. Excellent agreement is observed. It is seen that the variation of the first-mode eigenvalues due to uncertain modulus of elasticity existing in the right quarter of the plate is very small even if the second-order approach is used. However, the uncertain mass density existing in the right quarter has a significant effect on the variation of the first-mode eigenvalue. Furthermore, an obvious discrepancy between the results obtained by the first- and second-order approaches is seen when the random variable α_2 becomes larger than, say, 0.25 or smaller than, say, -0.25.

Vibration of a Simply Supported Laminated Plate with Uncertain Fiber Orientation in the First Lamina

The free vibration of a three-ply (60 deg/30 deg/0 deg) carbon/epoxy laminated rectangular plate, as shown in Fig. 2, with uncertain fiber orientation in the first lamina was studied. The rectangular plate was assumed to be simply supported at all edges with a length of 15.75 in., a width of 7.87 in., and a thickness for each lamina of 0.00787 in. The

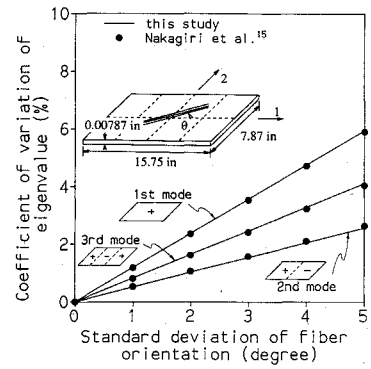

Fig. 2 Coefficients of variation of eigenvalues for the first three modes of a simply supported carbon/epoxy laminated (60 deg/30 deg/0 deg) rectangular plate with uncertain fiber orientation in the first lamina.

material properties of each lamina were assumed to be $E_L = 15.2 \times 10^6$ psi, $E_T = 1.27 \times 10^6$ psi, $\nu_{LT} = 0.327$, and $\rho = 0.144 \times 10^{-3}$ lb-s^2/in.^{4}.

A 4×2 finite element mesh was used to model the whole plate. Figure 2 shows the results for the coefficients of variation (COV) of eigenvalues for the first three modes, with different standard deviations (σ) of the fiber orientation in the first lamina. This problem was previously studied by Nakagiri et al.[15] using 64 plate elements. Their results are also plotted in Fig. 2 for comparison. Good agreement is observed. It is seen that the coefficients of variation of the second mode (antisymmetric mode) due to the uncertain fiber orientation in the first lamina are smaller than those of the first and third modes (symmetric modes).

Buckling and Reliability of a Simply Supported Laminated Square Plate with Structural Uncertainties

The buckling and reliability of an eight-ply $(\theta_1/\theta_2/\theta_3/\theta_4)_s$ graphite/epoxy laminated square plate were investigated. In this study the variability of volume fraction of fibers was accounted for by using the modulus of elasticity as a random variable. The orientation of fibers is considered as a separate random variable. The other structural uncertainties include thickness of each lamina and initial geometric imperfections over the entire plate.

The square plate was assumed to be simply supported with a length of 10 in. The mean value and coefficient of variation for the thickness of each lamina were assumed to be 0.005 in. and 5% respectively. The material of each lamina was assumed to be graphite/epoxy with $E_L = 20 \times 10^6$ psi, $E_T = 1.5 \times 10^6$ psi, $G_{LT} = 0.75 \times 10^6$ psi. and $\nu_{LT} = 0.25$. The coefficient of variation of the modulus of elasticity was assumed to be 5%, based on tests for over 500 samples by Delmonte.[30] The mean values of fiber orientation θ_i $(i = 1, \ldots, 4)$ were assumed to be 90, 45, -45, and 0 deg, respectively. The standard deviation of fiber orientation of lamina was assumed to be 2 deg.

The standard deviation of the random initial geometric imperfections was assumed to be $0.05h$, i.e., $\sigma\{w_0(x,y)/h\} = 5\%$, where $w_0(x,y)$ was the geometric function of imperfections. The following double Fourier series were used to discretize such a random field:

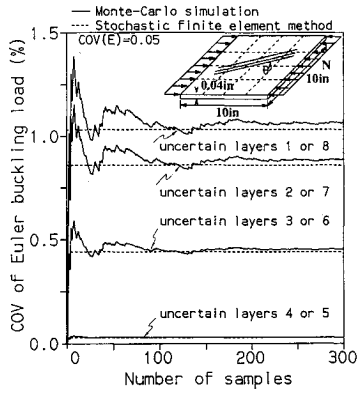

Fig. 3 Coefficients of variation of the Euler buckling load of a simply supported graphite/epoxy laminated (90 deg/45 deg/ − 45 deg/0 deg)$_s$ square plate with uncertain moduli of elasticity.

$$w_0(x,y) = \sum_{m=1}^{\infty} \sum_{n=1}^{\infty} \mu_{mn} \sin \frac{m\pi x}{L} \sin \frac{n\pi y}{L} \tag{21}$$

where the Fourier coefficients μ_{mn} are random variables. The covariance of these random variables can be obtained using Euler formulas.

A 4×4 finite element mesh was used to model the whole square plate. The coefficients of variation of the Euler buckling load due to the uncertain modulus of elasticity, thickness, fiber orientation in each lamina, and initial imperfections of the entire plate were obtained using the stochastic finite element method proposed in this study and shown in Tables 1 and 2. Since no alternative solutions are available to evaluate the stochastic finite element solutions, the Monte Carlo simulation approach using 300 samples was performed. Figure 3 shows the results for coefficients of variation of buckling loads due to the uncertain modulus of elasticity obtained by both methods. Goods agreement is seen. Other Monte Carlo simulation results are shown in Tables 1 and 2 with good agreements. It is seen that the uncertainties in the first (or eighth) lamina have the most significant effect on the variation of the buckling load.

Table 1 Coefficients of variation of the Euler buckling loads (mean value = 16.82 lb/in.) of a simply supported graphite/epoxy laminated (90 deg/45 deg/ − 45 deg/0 deg)$_s$ square plate with uncertain modulus of elasticity, thickness, and fiber orientation

Structural uncertainty	COV of Euler buckling values, %					
	Uncertain lamina				Zero correlation	Full correlation
	1 or 8	2 or 7	3 or 6	4 or 5		
Modulus of elasticity COV(E) = 5%	1.03 (1.07)[a]	0.86 (0.89)	0.44 (0.45)	0.03 (0.03)	2.00 (2.07)	4.71 (4.88)
Thickness COV(h) = 5%	1.16 (1.23)	0.85 (0.88)	0.42 (0.45)	0.02 (0.03)	2.12 (2.23)	4.91 (5.18)
Fiber orientation $\sigma(\theta) = 2$ deg	0.39 (0.38)	0.02 (0.02)	0.01 (0.01)	0.01 (0.01)	0.55 (0.54)	0.86 (0.84)

[a]Values shown in parentheses were obtained by Monte Carlo simulation.

Table 2 Coefficients of variation of the Euler buckling loads (mean value = 16.82 lb/in.) of a simply supported graphite/epoxy laminated (90 deg/45 deg/ − 45 deg/0 deg)$_s$

Structural uncertainty	COV of Euler buckling values, %				
	$m, n = 1$	$m, n = 1, 2$	$m, n = 1, \ldots, 3$	$m, n = 1, \ldots, 4$	$m, n = 1, \ldots, 5$
Geometric imperfection $\sigma(w_0/h) = 5\%$	1.62 (1.66)[a]	1.98 (2.04)	2.12 (2.20)	2.20 (2.30)	2.21 (2.32)

[a]Values shown in parentheses were obtained by Monte Carlo simulation.

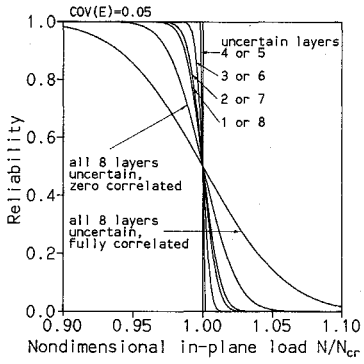

Fig. 4 Reliability of the simply supported graphite/epoxy laminated (90 deg/45 deg/ − 45 deg/0 deg)$_s$ square plate under uniform compression with uncertain moduli of elasticity.

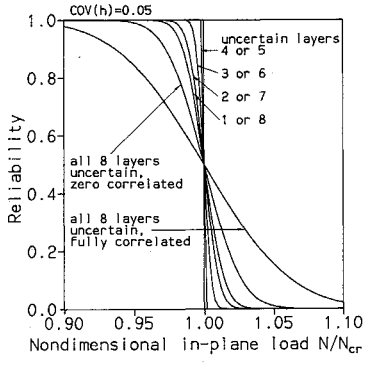

Fig. 5 Reliability of the simply supported graphite/epoxy laminated (90 deg/45 deg/ − 45 deg/0 deg)$_s$ square plate under uniform compression with uncertain thickness.

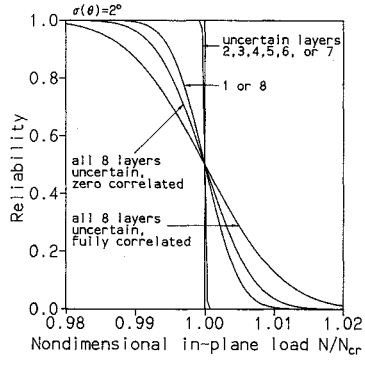

Fig. 6 Reliability of the simply supported graphite/epoxy laminated (90 deg/45 deg/ − 45 deg/0 deg)$_s$ square plate under uniform compression; with uncertain fiber orientations.

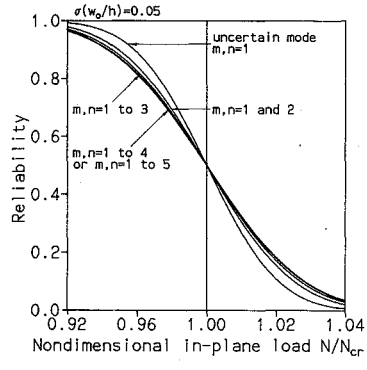

Fig. 7 Reliability of the simply supported graphite/epoxy laminated (90 deg/45 deg/ − 45 deg/0 deg)$_s$ square plate under uniform compression with random imperfections.

Based on the mean value of the buckling load and the standard deviation or coefficient of variation as shown in Tables 1 and 2, Gaussian distribution curves were obtained for each of the uncertain structural parameters. Structural reliability for a given in-plane load and a specific uncertain parameter could be obtained by integrating the portion of the area on the right-hand side of the given in-plane load and under the Gaussian distribution curve. The reliability curves thus obtained for uncertain modulus of elasticity, thickness, fiber orientation, and imperfection are plotted in Figs. 4, 5, 6, and 7, respectively.

It is seen in Figs. 4–6 that the reliability boundaries are lower when each random parameter occurred in the outer laminae. The reliability boundaries are farther down as the random parameters in all laminae are zero correlated. They become the lowest as the random parameters in all laminae are fully correlated. Figure 7 shows the reliability boundaries of the plate with random imperfections calculated including various modes. It is seen that the reliability values converge when 16 modes ($m, n = 1, \ldots, 4$) are considered and the first mode ($m = n = 1$) has a dominant effect on reducing the structural reliability.

In practical application it is possible that all of the previously given uncertain parameters occur simultaneously in a certain random fashion. Figure 8 shows the combined effects of all of these uncertain parameters on the structural reliability boundaries for the subject plate under in-plane compression. Two sets of coefficient of variation (or standard deviations) of the structural uncertainties were assumed, as listed in Fig. 8, to cover ranges of practical significance. Two extreme conditions, zero and full correlations, among these structural uncertainties were assumed. It is of interest to observe these curves by choosing a given value of structural reliability, say, 0.95. For this reliability value the allowable nondimensional in-plane compression decreases to 0.94 and 0.79 for the zero and fully correlative conditions, respectively, for case 1, and to 0.88 and 0.57, respectively, for case 2. A significant reduction of the allowable in-plane load of the uncertain plate is seen.

Supersonic Flutter and Reliability of a Simply Supported Laminated Square Plate with Structural Uncertainties

It is of interest to study the reliabilities of the present plate, which is the same as that of the previous example, considering supersonic flutter as a failure criterion. The same structural uncertain parameters were considered but with the addition of a mass density. The mean value and coefficient of variation for the mass density of each lamina were assumed to be 0.145×10^{-3} lb-s^2/in.^{4} and 5%, respectively. The aerodynamic pressure due to supersonic potential flow was based on the two-dimensional quasisteady supersonic theory, or the piston theory.[2] This theory is valid only when the Mach number is

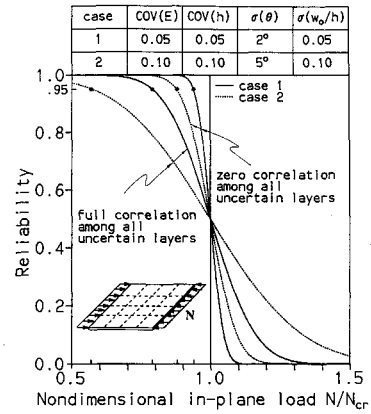

case	COV(E)	COV(h)	σ(θ)	σ(wo/h)
1	0.05	0.05	2°	0.05
2	0.10	0.10	5°	0.10

Fig. 8 Reliability of the simply supported graphite/epoxy laminated (90 deg/45 deg/ − 45 deg/0 deg)$_s$ square plate under uniform compression with four uncertain parameters.

beyond 1.6. In order to study the effect of randomness of airflow on the determination of flutter characteristic, the density of air was considered as an additional uncertain parameter.

A 4×4 finite element mesh was used to model the whole plate as shown in Fig. 9. As a first step, a deterministic analysis was performed to obtain the mean value of the flutter boundary. Since the effect of aerodynamic damping in the results for critical aerodynamics pressure for the present example cases was found to be within 3%, such an effect was thus neglected in all of the present stochastic analyses. The effect of the uncertain modulus of elasticity on the critical aerodynamic pressure was considered first. Figure 9 shows the coalescences of the mean, σ, 2σ, and 3σ bound values of the first- and second-mode frequencies due to uncertain moduli of elasticity $\{\mathrm{COV}(E)=0.05\}$. The nondimensional aerodynamic pressure β is defined as

$$\beta=\frac{2qa^3}{D(M_\infty^2-1)^{1/2}} \tag{22}$$

where q, M_∞, and D are the dynamic pressure and Mach number of the freestream, and the flexural rigidity of the plate, respectively. It is seen that the nondimensional critical aerodynamic pressures for the σ, 2σ, and 3σ bound values are reduced from the mean value of 116.367 to 115.224, 113.994, and 112.851, for the zero correlative condition, respectively, and also to 113.642, 110. 918, and 108.105, for the fully correlative condition, respectively. The fully correlative condition obviously has a more pronounced effect on reducing the critical aerodynamic pressure than the zero correlative condition.

In this example the reliability criterion was assumed as the probability of a given aerodynamic pressure to be less than the critical aerodynamic pressure. The reliability curves for the plate due to uncertain moduli of elasticity, thickness

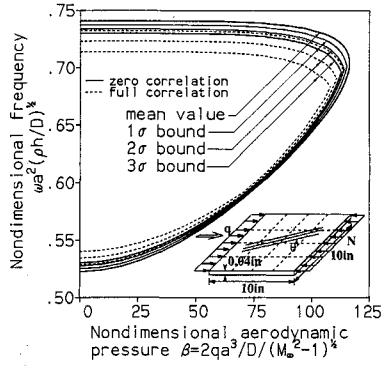

Fig. 9 Coalescence of the frequencies of the simply supported graphite/epoxy laminated (90 deg/45 deg/ − 45 deg/0 deg)$_s$ square plate with uncertain moduli of elasticity in all laminae.

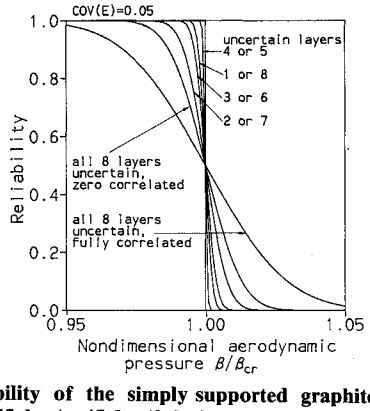

Fig. 10 Reliability of the simply supported graphite/epoxy laminated (90 deg/45 deg/ − 45 deg/0 deg)$_s$ square plate in supersonic flow with uncertain moduli of elasticity.

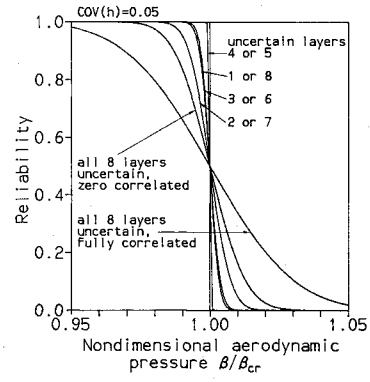

Fig. 11 Reliability of the simply supported graphite/epoxy laminated (90 deg/45 deg/ − 45 deg/0 deg)$_s$ square plate in supersonic flow with uncertain thickness.

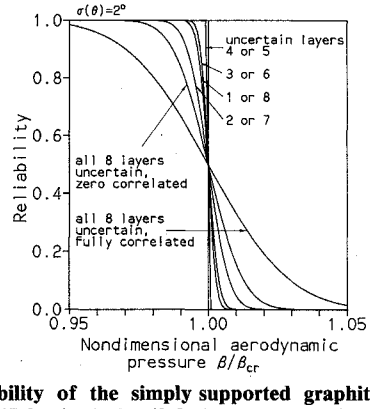

Fig. 12 Reliability of the simply supported graphite/epoxy laminated (90 deg/45 deg/ − 45 deg/0 deg)$_s$ square plate in supersonic flow with uncertain fiber orientations.

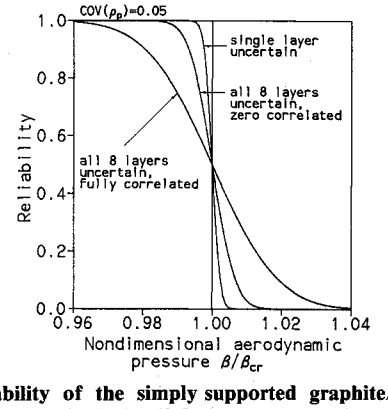

Fig. 13 Reliability of the simply supported graphite/epoxy laminated (90 deg/45 deg/ − 45 deg/0 deg)$_s$ square plate in supersonic flow with uncertain mass density.

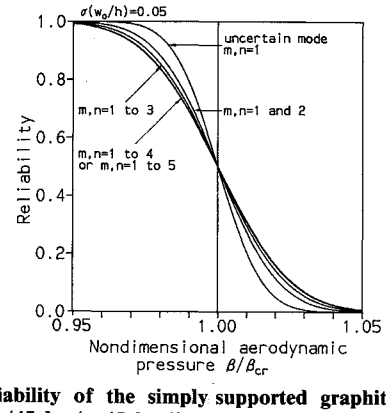

Fig. 14 Reliability of the simply supported graphite/epoxy laminated (90 deg/45 deg/ − 45 deg/0 deg)$_s$ square plate in supersonic flow with random imperfections.

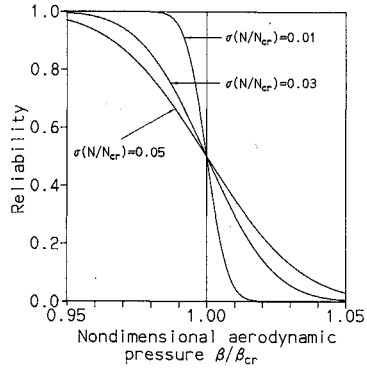

Fig. 15 Reliability of the simply supported graphite/epoxy laminated (90 deg/45 deg/ − 45 deg/0 deg)$_s$ square plate in supersonic flow under uniformly distributed random in-plane loads.

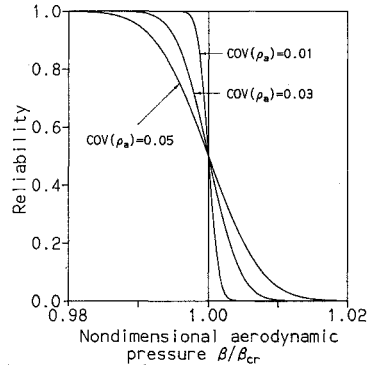

Fig. 16 Reliability of the simply supported graphite/epoxy laminated (90 deg/45 deg/ − 45 deg/0 deg)$_s$ square plate in supersonic flow with uncertain air density.

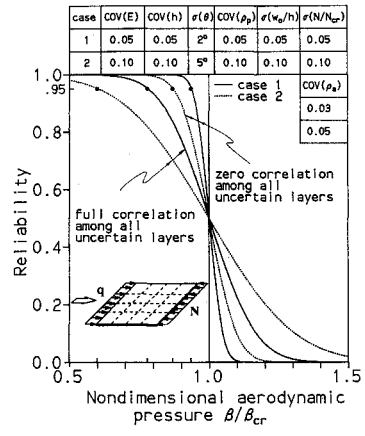

Fig. 17 Reliability of the simply supported graphite/epoxy laminated (90 deg/45 deg/ − 45 deg/0 deg)$_s$ square plate in supersonic flow with seven uncertain parameters.

{COV(h) = 0.05}, fiber orientation {$\sigma(\theta) = 2$ deg}, and mass density {COV(ρ_p) = 0.05} in each and all laminae were obtained and plotted in Figs. 10–13, respectively. It is seen that in Figs. 10–12 the reliability boundaries due to uncertain modulus of elasticity, thickness, and fiber orientation in each lamina are the lowest as each random parameter occurred in the second and seventh laminae ($\theta = 45$ deg). This observation is different from that found in the case of buckling analyses (Figs. 4–6), where the reliability boundaries are the lowest as each random parameter occurred in the first and eighth laminae ($\theta = 90$ deg). Obviously, the reliability is not only dominated by the location of the lamina along the thickness but also by the fiber orientation of the lamina. However, the reliability boundaries due to uncertain mass density in each lamina are identical. The reliability boundaries are farther down as the

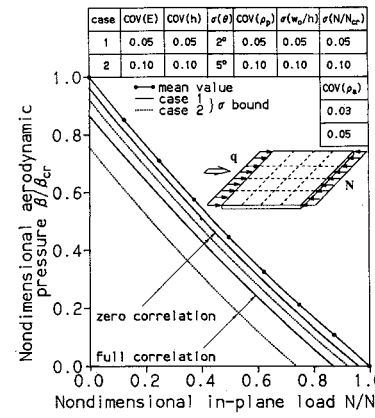

Fig. 18 Interactive effects between uniform compression and aerodynamic pressure for the simply supported graphite/epoxy laminated (90 deg/45 deg/ − 45 deg/0 deg)$_s$ square plate with seven uncertain parameters.

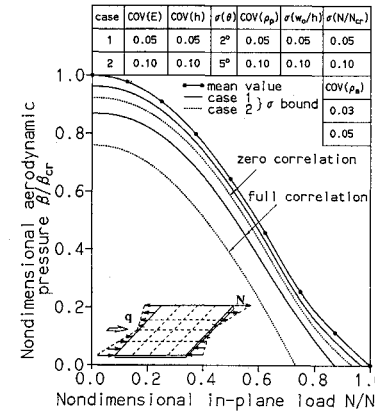

Fig. 19 Interactive effects between linearly distribution in-plane load and aerodynamic pressure for the simply supported graphite/epoxy laminated (90 deg/45 deg/ − 45 deg/0 deg)$_s$ square plate with seven uncertain parameter.

random parameters in all laminae are zero correlated. They become the lowest as the random parameters in all laminae are fully correlated. Figure 14 shows the reliability boundaries of the plate with random imperfections. It is seen that the reliability values converge when 16 modes ($m, n = 1, \ldots, 4$) are considered and the first mode ($m = n = 1$) has a dominate effect on reducing the structural reliability. Figure 15 shows the reliability boundary of the plate with random air density {COV(ρ_a) = 0.01, 0.03, and 0.05}. It is seen that the uncertain air density has an effect on reducing the structural reliability.

For a more practical application the effect of a random but uniformly distributed in-plane load was also considered. The mean value for the uniformly distributed random in-plane load could be assumed to be any value between zero and the Euler buckling load (N_{cr}). As will be seen in later figures, nine different mean values ($N/N_{cr} = 0$, 0.125, 0.25, 0.375, 0.5, 0.625, 0.75, 0.875, and 1) were assumed when the interactive effects between the in-plane load and aerodynamic pressure were studied. For this example the mean value was initially assumed to be zero. Figure 16 shows the reliability curves of the plate under uniformly distributed zero-mean random in-plane loads with different standard deviations, $\sigma(N/N_{cr}) = 0.01$, 0.03, and 0.05. It is seen that the uncertain in-plane load has an obvious effect on reducing the structural reliability.

Figure 17 shows the combined effects of all these uncertain parameters on the structural reliability of the plate in supersonic flow. Two sets of coefficients of variation (or standard deviations) of the uncertainties were assumed, as listed in Fig. 17. Two extreme conditions, zero and full correlations, among

these uncertainties were also assumed. It is interesting to see these curves by choosing a given value of structural reliability, say, 0.95. For this reliability value the allowable nondimensional aerodynamic pressure decreases to 0.94 and 0.78 for the zero and fully correlative conditions, respectively, for case 1, and to 0.87 and 0.60, respectively, for case 2. A significant reduction of the allowable aerodynamic pressure of the uncertain plate is observed.

Supersonic Flutter of a Simply Supported Laminated Square Plate with Structural Uncertainties Under Uniform and Linear, Nonzero-Mean, Random In-Plane Loads

In order to study the interactive effects between the in-plane load and aerodynamic pressure, the same plate was further studied by including the random effect of nonzero-mean in-plane loads. The mean values of the in-plane loads were varied from zero to its Euler buckling load N_{cr}. Two sets of coefficients of variation (or standard deviations) for all of the seven uncertain parameters were assumed, as listed in Fig. 18. Both zero and full correlative conditions among all the uncertainties were considered.

Figure 18 shows the mean values and the standard deviations of the critical aerodynamic pressure of the plate with the two sets of uncertain parameter values under uniformly distributed in-plane loads in the form of interactive stability boundaries. The effects of these random parameters with presently assumed values on the reduction of these stability boundaries were quantified in Fig. 18. It is apparent that, for case 2 and full correlation, this boundary is significantly reduced. It is of interest to note that the relationship between the critical aerodynamic pressure and the uniformly distributed in-plane load is approximately linear.

The random effect of linear distributed in-plane load was also considered. Figure 19 shows the mean values and standard deviations of the critical aerodynamic pressure of the plate with the two sets of uncertain parameter values under linearly distributed random in-plane loads. Again, the effects of the presently assumed random parameters on the reduction of the stability boundaries were quantified. It is interesting to see that the relationship between the critical aerodynamic pressure and the linearly distributed in-plane load is now obviously nonlinear. It is also of interest to point out that, for the present numerical method, the prediction for such nonlinear stability boundaries is as straightforward as that for the linear boundaries.

Concluding Remarks

A 16-DOF quadrilateral stochastic laminated thin-plate element with probabilistic modulus of elasticity, mass density, thickness, fiber orientations, geometric imperfections, in-plane loads, and air density has been formulated. The solution procedure was based on the mean-centered second-moment perturbation technique. The effects of these uncertain parameters on the vibration, buckling, supersonic flutter, and reliability have been studied.

The present results have been compared with alternative solutions in the case of vibration analyses (Figs. 1 and 2). A Monte Carlo simulation method has also been used to verify a set of coefficients of variation for Euler buckling loads (Tables 1 and 2).

In this study ranges of values for each random parameter were assumed, and the results obtained quantify the effects of these parameters on the reliabilities of the present laminated plates subjected to in-plane force and aerodynamic pressure.

The interactive effects between the in-plane load and aerodynamic pressure were also studied and quantified for the present sets of assumed random parameters. Such interactive stability boundaries were shown to be linear when the in-plane load was uniformly distributed and quite nonlinear when the in-plane load was linearly distributed.

These quantified data may have provided structural designers with some physical insight into the possible individual and combined effects of all these uncertain parameters. Such physical insight and quantified feelings may be helpful in their design of more reliable laminated composite plate structures.

The present formulation and solution procedure are general and simple so that extensions can be made to include some more interesting effects, such as transverse shear deformations for thicker plates, structural and aerodynamic dampings, as well as a structural and aerodynamic nonlinearities.

Acknowledgments

This study was sponsored by National Science Foundation Grant ECE-8516915. Technical guidance from M. P. Gaus and S. C. Liu is acknowledged.

References

[1]Mei, C., and Yang, T. Y., "Free Vibrations of Finite Element Plates Subjected to Complex Middle-Plane Force Systems," *Journal of Sound and Vibration*, Vol. 23, No. 2, 1972, pp. 145–156.

[2]Bisplinghoff, R. L., and Ashley, H., *Principles of Aeroelasticity*, Wiley, New York, 1962.

[3]Sander, G., Bon, C., and Geradin, M., "Finite Element Analysis of Supersonic Panel Flutter," *International Journal for Numerical Methods in Engineering*, Vol. 7, No. 3, 1973, pp. 379–394.

[4]Yang, T. Y., and Han, A. D., "Flutter of Thermally Buckled Finite Element Panels," *AIAA Journal*, Vol. 14, No. 7, 1976, pp. 975–976.

[5]Bolotin, V. V., "Statistical Method in the Nonlinear Theory of Elastic Shells," NASA TTF-85, 1962.

[6]Amazigo, J. C., "Buckling under Axial Compression of Long Cylindrical Shells with Random Axisymmetric Imperfections," *Quarterly Applied Mathematics*, Vol. 26, No. 4, 1969, pp. 537–566.

[7]Amazigo, J. C., "Asymptotic Analysis of the Buckling of Externally Pressurized Cylinders with Random Imperfections," *Quarterly Applied Mathematics*, Vol. 31, No. 4, 1974, pp. 429–442.

[8]Van Slooton, R. A., and Soong, T. T., "Buckling of a Long, Axially Compressed, Thin Cylindrical Shell with Random Initial Imperfections," *Journal of Applied Mechanics*, Vol. 39, No. 4, 1972, pp. 1066–1071.

[9]Dym, C. L., and Hoff, N. J., "Perturbation Solutions of the Buckling Problems of Axially Compressed Thin Cylindrical Shells of Infinite of Finite Length," *Journal of Applied Mechanics*, Vol. 35, No. 4, 1968, pp. 754–762.

[10]Scher Fersht, R., "Buckling of Cylindrical Shells with Random Imperfections," *Thin Shell Structures: Theory, Experiment, and Design*, edited by Y. C. Fung, and E. E. Sechler, Prentice-Hall, Englewood Cliffs, NJ, 1974, pp. 325–341.

[11]Elishakoff, I., and Arbocz, J., "Reliability of Axially Compressed Cylindrical Shells with Random Axisymmetric Imperfections," *International Journal of Solids and Structures*, Vol. 18, No. 7, 1982, pp. 563–585.

[12]Elishakoff, I., and Arbocz, J., "Reliability of Axially Compressed Cylindrical Shells with General Non-Symmetric Imperfections," *Journal of Applied Mechanics*, Vol. 52, No. 1, 1985, pp. 122–128.

[13]Elishakoff, I., Van Manen, S., Vermenlen, P. G., and Arbocz, J., "First-Order Second-Moment Analysis of the Buckling of Shells with Random Imperfections," *AIAA Journal*, Vol. 25, No. 8, 1987, pp. 1113–1117.

[14]Lawrence, M., "A Finite Element Solution Technique for Plates of Random Thickness," *Finite Element Methods for Plate and Shell Structures*, Vol. 2, edited by T. J. R. Hughes, and E. Hinton, Pineridge Press, Swansea, UK, 1986, pp. 213–228.

[15]Nakagiri, S., Takabatake, H., and Tani, S., "Uncertain Eigenvalue Analysis of Composite Laminated Plates by the Stochastic Finite Element Method," *Journal of Engineering for Industry*, Vol. 109, No. 1, 1987, pp. 9–12.

[16]Kennedy, R. P., Cornell, C. A., Campbell, R. D., Kaplan, S., and Perla, H. F., "Probabilistic Seismic Safety Study of an Existing Nuclear Power Plant," *Nuclear Engineering and Design*, Vol. 59, No. 2, 1980, pp. 315–338.

[17]Smith, P. D., Dong, R. G., Bernreuter, D. L., Bohn, M. P., Chang, T. Y., Cummings, G. E., Johnson, J. J., Mensing, R. W., and Wells, J. E., "Seismic Safety Margins Research Program Phase I Final Report-Overview," NUREG/CR-2015, Vol. 1, UCRL-53021, Vol. 1, 1981.

[18]Vanmarcke, E., Shinozuka, M., Nakagiri, S., Schueller, G. I., and Grigoriu, M., "Random Fields and Stochastic Finite Elements," *Structural Safety*, Vol. 3, Nos. 3 and 4, 1986, pp. 143–166.

[19]Nakagiri, S., and Hisada, T., *An Introduction to Stochastic Finite Elements*, Baifukan, Tokyo, 1987, (in Japanese).

[20]Librescu, L., and Badoiu, T., "On the Supersonic Flutter of Rectangular Anisotropic, Heterogeneous Flat Structures," NASA TT-F-15, 890, 1974.

[21]Librescu, L., "Aeroelastic Stability of Orthotropic Heterogeneous Thin Panels in the Vicinity of the Flutter Critical Boundary (I)," *Journal de Mecanique*, Vol. 4, No. 1, 1965, pp. 51–76.

[22]Librescu, L., "Aeroelastic Stability of Orthotropic Heterogeneous Thin Panels in the Vicinity of the Flutter Critical Boundary (II)," *Journal de Mecanique*, Vol. 6, No. 1, 1967, pp. 133–152.

[23]Han, A. D., and Yang, T. Y., "Nonlinear Panel Flutter Using High-Order Triangular Finite Elements," *AIAA Journal*, Vol. 21, No. 10, 1983, pp. 1453–1461.

[24]Zienkiewicz, O. C., *The Finite Element Method*, 3rd ed., McGraw-Hill, London, UK, 1977.

[25]Liaw, D. G., "Stochastic Finite Element Analysis of Uncertain Structures," Ph.D. Dissertation, Purdue University, West Lafayette, IN, Dec. 1990.

[26]Fox, R. L., and Kapoor, M. P., "Rates of Change of Eigenvalues and Eigenvectors," *AIAA Journal*, Vol. 6, No. 12, 1968, pp. 2426–2429.

[27]Collins, J. D., and Thomson, W. T., "The Eigenvalue Problem for Structural Systems with Statistical Properties," *AIAA Journal*, Vol. 7, No. 4, 1969, pp. 642–648.

[28]Rudisill, C. S., "Derivatives of Eigenvalues and Eigenvectors for a General Matrix," *AIAA Journal*, Vol. 12, No. 5, 1974, pp. 721–722.

[29]Nakagiri, S., and Hisada, T., "Stochastic Finite Element Method Applied to Eigenvalue Analysis of Uncertain Structural System" *Transactions of the Japan Society of Mechanical Engineers,* Series A, Vol. 49, No. 438, 1983, pp. 239–246.

[30]Delmonte, J., *Technology of Carbon and Graphite Fiber Composites*, Van Nostrand Reinhold, New York, 1981.